Coupled-channel scattering in 1+1 dimensional lattice model

Peng Guo

Phys. Rev. D **88**, 014507 — Published 8 July 2013

DOI: 10.1103/PhysRevD.88.014507

Coupled-channel scattering in $1+1$ dimensional lattice model

Peng Guo[1,*]

[1] *Thomas Jefferson National Accelerator Facility, Newport News, VA 23606, USA*

Based on the Lippmann-Schwinger equation approach, a generalized Lüscher's formula in $1+1$ dimensions for two particles scattering in both the elastic and coupled-channel cases in moving frames is derived. A 2D coupled-channel scattering lattice model is presented, the model represents a two-coupled-channel resonant scattering scalars system. The Monte Carlo simulation is performed on finite lattices and in various moving frames. The 2D generalized Lüscher's formula is used to extract the scattering amplitudes for the coupled-channel system from the discrete finite-volume spectrum.

PACS numbers: 11.80.Gw, 13.75.Lb,12.38.Gc
Keywords:

I. INTRODUCTION

In recent years, remarkable progresses have been made on hadrons scattering in lattice QCD from both the theoretical algorithm of extracting scattering amplitudes from lattice data [1–7, 9–13] and the practical lattice QCD computational algorithm aspect [14–18]. Since Lüscher proposed the elastic scattering formalism in a finite volume [1], the framework has been quickly extended to moving frames [2–6], and to coupled-channel scattering [7–13]. The finite volume scattering formalism has been successfully used by the lattice community to extract elastic hadron-hadron scattering phase shifts [19–27]. Realistic lattice QCD computations on coupled-channel hadron-hadron scattering are under way.

For the purpose of demonstrating the feasibility of extracting coupled-channel scattering amplitudes from lattice data and discussing some issues, such as, finite size effects, in this work, we present a coupled-channel scattering lattice model in 2D. Our model is a direct generalization of a 2D single channel scattering lattice model in [28]. The advantage of scattering in 2D is that only finite numbers of scattering amplitudes contribute in one spatial dimensional scattering theory, and the relation between phase shift and energy level in Lüscher's formula in 2D [15] appears more transparent. Our 2D lattice model represents a coupled-channel resonant scattering system with three species of scalar fields (ϕ, σ, ρ), where the scalar field ρ acts as a resonance which couples to both 2ϕ and 2σ channels. The Monte Carlo simulation are carried out on various lattice sizes and in different moving frames. We also present the derivation of 2D Lüscher's formulae in a general moving frame and for a coupled-channel system. The derivation is based on the Lippmann-Schwinger equation approach presented in [13]. These formulae are used in the end to extract the scattering amplitudes from Monte Carlo simulation data. The finite size effect on extracting scattering amplitudes (phase shifts and inelasticity) from lattice data is also addressed in this work. Although, our model is formulated and computed in $1+1$ dimensions, it still captures many of the features of hadrons scattering in a real $3+1$ dimensional QCD computation, and sheds some light on the future coupled-channel hadron-hadron scattering lattice QCD calculation.

The paper is organized as follows. A discussion of elastic scattering in a finite volume is given in Section II, with extension to the coupled channel system in Section III. The 2D lattice model, the Monte Carlo simulation and data analysis are described in Section IV. The summary and outlook are given in Section V.

II. LUSCHER'S FORMULA IN $1+1$ DIMENSIONS

For completeness, we first present the basic scattering theory in $1+1$ dimensions. Based on the Lippmann-Schwinger equation approach, a generalized Lüscher's formula in $1+1$ dimensions for two particles elastic scattering in moving frames is presented in the end of this Section.

A. Two-particle scattering in infinite volume

We consider spinless particles scattering in a symmetric potential $\tilde{V}(-x) = \tilde{V}(x)$, the mass of scalar particles is m and x is relative coordinate of two particles. The wave function of scattering particles in center of mass frame satisfies the relativistic Lippmann-Schwinger equation

$$\psi(x) = \int_{-\infty}^{\infty} dx' G_0(x - x'; \sqrt{s}) \tilde{V}(x') \psi(x'), \qquad (1)$$

where the center of mass frame energy is $\sqrt{s}$, and the free-particle Green's function is given by

$$G_0(x; \sqrt{s}) = \int_{-\infty}^{\infty} \frac{dq}{2\pi} \frac{e^{iqx}}{\sqrt{s} - 2\sqrt{q^2 + m^2}}. \qquad (2)$$

*Electronic address: pguo@jlab.org

The Green's function can be further written as a oscillating term and an exponentially decaying term over the separation of two particles. The singularities of integrand in Eq.(2) on the complex q plane are two poles on real axis $q = \pm k$ and two branch cuts on imaginary axis $\pm\,[im, i\infty]$, see Fig.1. Therefore, for $x > 0$, we choose the contour $C_1 + C_2$ to include pole $q = k$ and cross the cut $[im, i\infty]$, and for $x < 0$, we choose the contour $C_1 + C_3$ to include pole $q = -k$ and cross the cut $-\,[im, i\infty]$, as shown in Fig.1. Thus, contour integral leads to

$$G_0(x, \sqrt{s}) = -i\frac{\sqrt{s}}{4k}e^{ik|x|} - \int_m^\infty \frac{d\rho}{2\pi}\sqrt{\rho^2 - m^2}\,\frac{e^{-\rho|x|}}{k^2 + \rho^2}, \tag{3}$$

where $k = \frac{\sqrt{s-4m^2}}{2}$ is momentum of particle in CM frame. At large separations, the free Green's function can be approximated by the oscillating term only

$$G_0(x - x', \sqrt{s}) \overset{|x|>|x'|}{\simeq} -i\frac{\sqrt{s}}{4k}e^{ik|x|}\sum_{\mathcal{P}=\pm} Y_{\mathcal{P}}(x)Y_{\mathcal{P}}(x')J^*_{\mathcal{P}}(kx'), \tag{4}$$

where the functions $Y_{\mathcal{P}}(x)$ and $J_{\mathcal{P}}(kx)$ are defined by

$$Y_+(x) = 1, \quad Y_-(x) = \frac{x}{|x|}, \tag{5}$$

$$J_+(kx) = \cos k|x|, \quad J_-(kx) = i\sin k|x|. \tag{6}$$

Such that $Y_{\mathcal{P}}(x)$ and $J_{\mathcal{P}}(kx)$ resemble the spherical harmonic and Bessel functions in three spatial dimensions, and $Y_{\mathcal{P}}(x)$ is the parity eigenstate with eigenvalue $\mathcal{P}$. The continuous rotation symmetry in three dimensions reduces to discrete spatial reflection $x \to -x$ in one spatial dimension, thus, the partial wave expansion of wave function in three dimensions reduce to the expansion of the wave function in terms of parity eigenstates $\psi(x) = \sum_{\mathcal{P}=\pm} c_{\mathcal{P}}\psi_{\mathcal{P}}(x)$, where $\psi_{\mathcal{P}}(-x) = \mathcal{P}\psi_{\mathcal{P}}(x)$.

For a potential $\tilde{V}$ which falls at large separations, Eq.(1) is solved outside the range of the potential by

$$\psi(x) \overset{|x|>R}{\longrightarrow} \sum_{\mathcal{P}=\pm} c_{\mathcal{P}}Y_{\mathcal{P}}(x)\left[J_{\mathcal{P}}(kx) + ie^{ik|x|}f_{\mathcal{P}}(k)\right], \tag{7}$$

where R denotes to the effective range of potential and the free solutions has been also included in Eq.(7). The scattering amplitudes are defined by

$$c_{\mathcal{P}}f_{\mathcal{P}}(k) = -\frac{\sqrt{s}}{4k}\int_{-\infty}^{\infty} dx' Y_{\mathcal{P}}(x')J^*_{\mathcal{P}}(kx')\tilde{V}(x')\psi(x'), \tag{8}$$

which up to the inelastic threshold can be parametrized by scattering phase shift

$$f_{\mathcal{P}}(k) = e^{i\delta_{\mathcal{P}}}\sin\delta_{\mathcal{P}}. \tag{9}$$

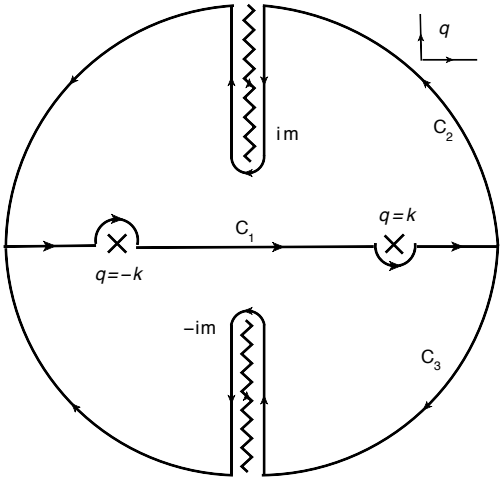

FIG. 1: The integration contours and singularities of free Green's function in Eq.(2) on complex q plane.

B. Two-particle scattering on a torus

Now we consider the theory in a one spatial dimensional box with periodic boundary conditions[1]. In lattice QCD calculations, the computations are usually done in the moving frame of the two-particle system [2]. After the system is boosted back to the CM frame, the shape of cubic box in moving frame is deformed in CM frame due to Lorentz contraction. Similarly, in the one spatial dimension, the volume of a one dimensional box, L, in a moving frame with total momentum $P = \frac{2\pi}{L}d, d \in \mathbb{Z}$ becomes γL in CM frame, where $\gamma = \sqrt{1 + \frac{P^2}{s}}$ is the Lorentz contraction factor.

Taking into account the Lorentz contraction effect as well, we divide the integral over x' into a sum of integrals over each translated box in Eq.(1), giving,

$$\psi^{(L)}(x) = \sum_{n\in\mathbb{Z}}\int_{-\frac{\gamma L}{2}}^{\frac{\gamma L}{2}} dx' G_0(x - x' - \gamma nL; \sqrt{s}) \times \tilde{V}(x' + \gamma nL)\psi^{(L)}(x' + \gamma nL). \tag{10}$$

The wave function in CM frame satisfies the boundary condition [2] of

$$\psi^{(L)}(x + \gamma nL) = e^{i\frac{P}{2}nL}\psi^{(L)}(x), \tag{11}$$

[1] The temporal extent of system has been assumed to be infinite large in Section II and III. In a real lattice simulation, the temporal extent of system is usually taken to be finite, but large enough so that the finite temperature corrections from the boundary of finite box in temporal direction can be neglected. The periodic or anti-periodic boundary condition in temporal direction is commonly applied to bosonic or fermionic system respectively, which guarantees the energy conservation of the system.

Using the periodicity of the potential $\tilde{V}(x'+\gamma nL) = \tilde{V}(x')$, we have

$$\psi^{(L,P)}(x) = \int_{-\frac{\gamma L}{2}}^{\frac{\gamma L}{2}} dx' G_P(x-x';\sqrt{s})\tilde{V}(x')\psi^{(L,P)}(x'), \tag{12}$$

where the periodic Green's function is given by

$$G_P(x-x';\sqrt{s}) = \sum_{n\in\mathbb{Z}} G_0(x-x'-\gamma nL;\sqrt{s})e^{i\frac{P}{2}nL}. \tag{13}$$

By using the Poisson summation formula, $\frac{1}{2\pi}\sum_{n\in\mathbb{Z}} e^{i\frac{P}{2}nL} = \frac{1}{\gamma L}\sum_{n\in\mathbb{Z}}\delta(\frac{P}{2\gamma} + \frac{2\pi}{\gamma L}n)$, Eq.(13) can be reexpressed as

$$G_P(x-x';\sqrt{s}) = \frac{1}{\gamma L}\sum_{q\in P_d}\frac{e^{iq(x-x')}}{\sqrt{s}-2\sqrt{q^2+m^2}}, \tag{14}$$

where $P_d = \{q\in\mathbb{R}|q = \frac{2\pi}{\gamma L}(n+\frac{d}{2}), \text{for } n\in\mathbb{Z}\}$.

As in the infinite volume case, the periodic Green's function Eq.(14) can be shown to consist of an oscillatory part and an exponentially decaying part which can be neglected for large volume $\gamma L > m^{-1}$. The remaining oscillatory part takes the form

$$G_P(x-x';\sqrt{s}) \to -i\frac{\sqrt{s}}{4k}\sum_{n\in\mathbb{Z}} e^{ik|x-x'-\gamma nL|}e^{i\frac{P}{2}nL}, \tag{15}$$

where we have used Eq.(3) and Eq.(13). The infinite sum in Eq.(15) can be done analytically, the details are presented in Appendix A, so that

$$\begin{aligned} &G_P(x-x';\sqrt{s}) \\ &\quad\overset{|x|>|x'|}{\simeq} -i\frac{\sqrt{s}}{4k}\sum_{\mathcal{P}=\pm} Y_{\mathcal{P}}(x)Y_{\mathcal{P}}(x')J^*_{\mathcal{P}}(kx') \\ &\qquad\times\left[e^{ik|x|} - \left(1 - i\cot\frac{\gamma kL+\pi d}{2}\right)J_{\mathcal{P}}(kx)\right]. \end{aligned} \tag{16}$$

Using the definition of scattering amplitudes in Eq.(8), we can express the wave function as

$$\begin{aligned} \psi^{(L,P)}(x) &\overset{|x|>R}{\longrightarrow} \sum_{\mathcal{P}=\pm} c_{\mathcal{P}}Y_{\mathcal{P}}(x)f_{\mathcal{P}}(k) \\ &\times\left[ie^{ik|x|} - \left(i + \cot\frac{\gamma kL+\pi d}{2}\right)J_{\mathcal{P}}(kx)\right]. \end{aligned} \tag{17}$$

Matching the wave function in finite box given by Eq.(17) to the wave function in infinite volume given by Eq.(7) at a arbitrary $|x| > R$, we obtain

$$\begin{aligned} &\sum_{\mathcal{P}=\pm} c_{\mathcal{P}}Y_{\mathcal{P}}(x)J_{\mathcal{P}}(kx)f_{\mathcal{P}}(k) \\ &\qquad\times\left[\frac{1}{f_{\mathcal{P}}(k)} + i + \cot\frac{\gamma kL+\pi d}{2}\right] = 0. \end{aligned} \tag{18}$$

which has non-trivial solution when

$$\cot\delta_{\mathcal{P}} + \cot\frac{\gamma kL+\pi d}{2} = 0. \tag{19}$$

III. COUPLED-CHANNEL SCATTERING IN $1+1$ DIMENSIONS

The previous discussion in section II can be generalized to a coupled channel system by including another species of scalar fields, let's name two species of particles ϕ and σ, the masses are $m_{\phi,\sigma}$. The coupled channel wave function has the form of $\psi(x) = \sum_{\alpha=\phi,\sigma}\psi^{\alpha}(x)$, and $\psi^{\alpha}(x)$ satisfies equation

$$\psi^{\alpha}(x) = \int_{-\infty}^{\infty} dx' G_0^{\alpha}(x-x';\sqrt{s})\sum_{\beta=\phi,\sigma}\tilde{V}_{\alpha\beta}(x')\psi^{\beta}(x'), \tag{20}$$

where Eq.(20) describes a $\phi\phi+\sigma\sigma \leftrightarrow \phi\phi+\sigma\sigma$ coupled-channel scattering system. A 2×2 matrix of coupled-channel scattering amplitudes can be defined by

$$c^{\alpha}_{\mathcal{P}}f^{\alpha\beta}_{\mathcal{P}} = -\frac{\sqrt{s}}{4k_{\alpha}}\int_{-\infty}^{\infty} dx' Y_{\mathcal{P}}(x')J^*_{\mathcal{P}}(k_{\alpha}x')\tilde{V}_{\alpha\beta}(x')\psi^{\beta}(x'), \tag{21}$$

where $k_{\alpha} = \frac{\sqrt{s-4m_{\alpha}^2}}{2}$ is the CM frame scattering momentum in channel α. Neglecting exponentially decaying terms and also include the free solution, we have for the wave function in channel α

$$\begin{aligned} \psi^{\alpha}(x) &\overset{|x|>R}{\longrightarrow} \sum_{\mathcal{P}=\pm} Y_{\mathcal{P}}(x) \\ &\times\left[c^{\alpha}_{\mathcal{P}}J_{\mathcal{P}}(k_{\alpha}x) + ie^{ik_{\alpha}|x|}\sum_{\beta} c^{\beta}_{\mathcal{P}}f^{\alpha\beta}_{\mathcal{P}}\right]. \end{aligned} \tag{22}$$

Extending the single channel derivation in finite-volume to the two-channel system, one obtains,

$$\begin{aligned} \psi^{\alpha(L,P)}(x) &\overset{|x|>R}{\longrightarrow} \sum_{\mathcal{P}=\pm}\sum_{\beta} c^{\beta}_{\mathcal{P}}Y_{\mathcal{P}}(x)f^{\alpha\beta}_{\mathcal{P}} \\ &\times\left[ie^{ik_{\alpha}|x|} - \left(i + \cot\frac{\gamma k_{\alpha}L+\pi d}{2}\right)J_{\mathcal{P}}(k_{\alpha}x)\right]. \end{aligned} \tag{23}$$

Matching the wave function in finite-volume, Eq.(23) to the wave function in infinite volume, Eq.(22), we can derive a condition for non-trivial solutions

$$\left(\frac{1}{f_{\mathcal{P}}^{\phi\phi}}+i+\cot\frac{\gamma k_\phi L+\pi d}{2}\right)\left(\frac{1}{f_{\mathcal{P}}^{\sigma\sigma}}+i+\cot\frac{\gamma k_\sigma L+\pi d}{2}\right)=\left(i+\cot\frac{\gamma k_\phi L+\pi d}{2}\right)\left(i+\cot\frac{\gamma k_\sigma L+\pi d}{2}\right)\frac{\left(f_{\mathcal{P}}^{\phi\sigma}\right)^2}{f_{\mathcal{P}}^{\phi\phi}f_{\mathcal{P}}^{\sigma\sigma}}. \tag{24}$$

The scattering amplitudes can be parametrized by three real parameters: two phase shifts $\delta_{\mathcal{P}}^{\alpha}$ and an inelasticity $\eta_{\mathcal{P}}$,

$$f_{\mathcal{P}}^{\alpha\alpha}=\frac{\eta_{\mathcal{P}}e^{2i\delta_{\mathcal{P}}^{\alpha}}-1}{2i}, f_{\mathcal{P}}^{\alpha\beta}=\frac{\sqrt{1-\eta_{\mathcal{P}}^2}e^{i\left(\delta_{\mathcal{P}}^{\alpha}+\delta_{\mathcal{P}}^{\beta}\right)}}{2}. \tag{25}$$

Thus, we can also write the Eq.(24) as

$$\eta_{\mathcal{P}}\left(-1\right)^d=\frac{\cos\left(\gamma L\frac{k_\phi+k_\sigma}{2}+\delta_{\mathcal{P}}^{\phi}+\delta_{\mathcal{P}}^{\sigma}\right)}{\cos\left(\gamma L\frac{k_\phi-k_\sigma}{2}+\delta_{\mathcal{P}}^{\phi}-\delta_{\mathcal{P}}^{\sigma}\right)}. \tag{26}$$

IV. THE ISING MODEL FOR COUPLED CHANNEL SCATTERING

To simulate a coupled channel scattering system, we build a model with two light mass fields (ϕ,σ) coupled to a heavier mass field ρ with two 3-point couplings, $\rho\phi^2$ and $\rho\sigma^2$. The physical masses of the fields are calibrated to be at the region $2m_\phi<2m_\sigma<m_\rho<4m_\phi$. For elastic scattering, the Ising model has been used and tested in both $1+1$ [28] and $3+1$ [2] dimensions by coupling two Ising fields, ϕ and ρ, together through a 3-point nonlocal interaction. For our purpose, we could introduce one more species of Ising field σ and another 3-point term to couple σ and ρ together, where ρ field gives rise to the resonant behavior in both $\phi\phi$ and $\sigma\sigma$ channels.

The action is given by

$$\begin{aligned}S=&-\sum_{\alpha=\phi,\sigma,\rho}\kappa_\alpha\sum_{x,\mu}\alpha(x)\alpha(x+\hat{\mu})\\&+\sum_{\beta=\phi,\sigma}g_{\rho\beta\beta}\sum_{x,\mu}\rho(x)\beta(x)\beta(x+\hat{\mu}),\end{aligned} \tag{27}$$

where $x=(x_0,x_1)$ is coordinates of Euclidean $T\times L$ lattice site and $\hat{\mu}$ denotes the unit vector in direction μ. The values of the fields are restricted to ±1, and the periodic boundary condition has been applied in Monte Carlo simulation. In the scaling limit, the Ising model represent a lattice ϕ^4 theory, thus, the action in Eq.(27) effectively describes an interacting theory of [2]

$$\begin{aligned}S=&\sum_{\alpha=\phi,\sigma,\rho}\int d^2x\left[\frac{1}{2}\left(\partial\alpha\right)^2+\frac{1}{2}m_\alpha^2\alpha^2+\frac{\lambda_\alpha}{4!}\alpha^4\right]\\&+\int d^2x\left(\frac{g_{\rho\phi\phi}}{2}\rho\phi^2+\frac{g_{\rho\sigma\sigma}}{2}\rho\sigma^2\right)\end{aligned} \tag{28}$$

in Euclidean space. By adjusting the masses and coupling constants, we could have an resonance ρ sit above both 2ϕ and 2σ thresholds, and couple to both channels by interaction terms $g_{\rho\phi\phi}\rho\phi^2$ and $g_{\rho\sigma\sigma}\rho\sigma^2$ respectively. Therefore, the lattice Monte Carlo simulation by using the action in Eq.(27) is expected to imitate a coupled-channel scattering model: $\phi\phi+\sigma\sigma\leftrightarrow\rho\leftrightarrow\phi\phi+\sigma\sigma$. Due to the Bose-symmetry, only scattering amplitudes with positive parity contribute in this model.

A. Cluster algorithm for coupled-channel Ising model

An generalized cluster algorithm is used in our simulation, similar to the cluster algorithm in [28], we update ρ, ϕ and σ fields alternately.

Updating the ρ field: Bonds between neighbored spins of equal sign are kept with the probability $1-e^{-2\kappa_\rho}$. After identification of the connected clusters, the spin of cluster is flipped with probability

$$p_\rho^{\text{flip}}=\frac{1}{1+e^{-2\alpha(C)}}, \tag{29}$$

$$\alpha(C)=\sum_{\beta=\phi,\sigma}g_{\rho\beta\beta}\sum_{x\in C,\mu}\rho(x)\beta(x)\beta(x+\hat{\mu}). \tag{30}$$

Updating the $\beta=\phi,\sigma$ fields: Bonds between like-sign neighbors are kept with the probability $1-e^{-2\left[\kappa_\beta-g_{\rho\beta\beta}\frac{\rho(x)+\rho(x+\hat{\mu})}{2}\right]}$, the spin of cluster is flipped with probability $\frac{1}{2}$.

In our simulation, the parameters are chosen as $\kappa_\rho=0.3323,\kappa_\phi=0.3897,\kappa_\sigma=0.3748$, and $g_{\rho\phi\phi}=g_{\rho\sigma\sigma}=0.02$, the masses of ϕ and σ fields are measured through single particle propagators, the values are given by $m_\phi\simeq0.176$ and $m_\sigma\simeq0.240$ respectively in lattice unit. The mass of resonance ρ is established from phase shifts, and the approximate value is given by $m_\rho\simeq0.57$.

In this work, we use $T=80$ and various spatial extent L between 15 and 50. For each set of lattice size and moving frame, we generated typically one million measurements.

B. Particles spectrum

As shown in the elastic scattering case in $1+1$ dimensions [28], one particle propagator can be constructed by operators

$$\tilde{\alpha}_n(x_0)=\frac{1}{L}\sum_{x_1}\alpha(x)e^{ix_1q_{1,n}}, \tag{31}$$

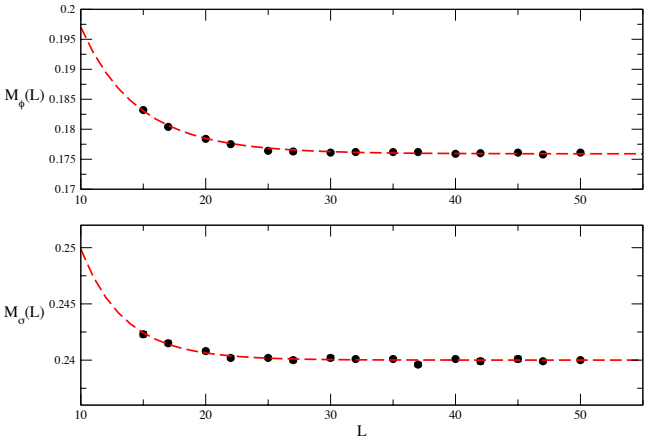

FIG. 2: $m_{\phi,\sigma}$ as function of L, they follow the function of $M_\alpha(L) = m_\alpha + c_\alpha/L^{1/2}e^{-m_\alpha L}$ (red dashed curves).

where $q_{1,n} = \frac{2\pi}{L}n, n = -L/2+1, \cdots, L/2$ and $\alpha = \phi, \sigma$. The spectrum of single particle fields is extracted from exponential decay of the correlation functions

$$C_{\alpha,n}(x_0) = \langle \tilde{\alpha}_{-n}(x_0)\tilde{\alpha}_n(0)\rangle \propto e^{-E_q^\alpha x_0}. \quad (32)$$

The single particle's masses satisfy relation $M_\alpha(L) = m_\alpha + c_\alpha L^{-1/2}e^{-m_\alpha L}$ [28], see Fig.2.

The two particles operators in the moving frame with total momentum of $P = \frac{2\pi}{L}d, d \in \mathbb{Z}$ are constructed from single particle operators

$$O^d_{(\rho,d)}(x_0) = \tilde{\rho}_d(x_0), \quad (33)$$
$$O^d_{(\alpha,n)}(x_0) = \tilde{\alpha}_n(x_0)\tilde{\alpha}_{d-n}(x_0). \quad (34)$$

The two particles correlation function matrices read

$$C^d_{ij}(x_0) = \langle \left[O^{d*}_i(x_0) - \delta_{d,0}O^{d*}_i(x_0+1)\right] O^d_j(0)\rangle, \quad (35)$$

where short hand notation i, j denotes the different sets of (ρ, d) or (α, n). The disconnected contribution has to be subtracted in CM frame ($d = 0$). The spectral decomposition of the correlation function matrices has the form,

$$C^d_{ij}(x_0) = \sum_l v^{(d,l)*}_i v^{(d,l)}_j e^{-E^{(d)}_l x_0}, \quad (36)$$

where $v^{(d,l)}_i = \langle l|O^d_i(0)|0\rangle$ and l labels the energy eigenstate $E^{(d)}_l$. The energy levels are determined by solving generalized eigenvalue problem [15]

$$C^d(x_0)\xi_l = \lambda_{(d,l)}(x_0, \bar{x}_0)C^d(\bar{x}_0)\xi_l, \quad (37)$$

where $\lambda_{(d,l)}(x_0, \bar{x}_0) = e^{-(x_0-\bar{x}_0)E^{(d)}_l}$ and $\bar{x}_0$ is a small reference time, in our analysis, $\bar{x}_0$ is set to be zero. In our simulation, the size of the matrices varies according to the volume, the number of operators we are using is always two or three more than the number of energy eigenstates in the region $2m_\phi < \sqrt{s} < 4m_\phi$. The values of the energy levels are determined by fitting $\lambda_{(d,l)}(x_0, 0)$ for $0 \leqslant x_0 \leqslant 6-10$ with the form

$$\lambda_{(d,l)}(x_0, 0) = \left(1 - A_{(d,l)}\right) e^{-m_{(d,l)}x_0} + A_{(d,l)}e^{-m'_{(d,l)}x_0},$$

where $A_{(d,l)}, m_{(d,l)}$ and $m'_{(d,l)}$ are fitting parameters. This form allows a second exponential, however, we found that the value of $m'_{(d,l)}$ is typically $2-3$ times of the value of $m_{(d,l)}$, so that it decreases rapidly and the first exponential becomes dominant at around $x_0 = 2$. It is worth to mention that, in a real $3+1$ dimensional lattice simulation, for certain systems, such as, the nucleon-nucleon (NN) system, the splitting between ground and 1st excited states may be as small as $40-50$ MeV [29]. Thus, the contaminations from excited states may persist up to a large x_0 in correlation functions, unfortunately, the signal-to-noise ratio for the correlation function of such system is usually problematic statistically at large x_0 [29], so that extracting signals at large x_0 becomes extremely difficult. In those cases, the alternative techniques may be required, for a example, the method developed by HAL QCD Collaboration for nucleon-nucleon (NN) system [29].

We show the measured two-particle energy spectra from our simulations in Fig.3 for various volumes and total momenta of two particles system $P = \frac{2\pi}{L}d, d = 0, 1, 2$.

C. A coupled-channel K-matrix model

In order to extract the scattering amplitudes (phase shifts and inelasticity) from the discrete finite volume spectra of the Monte Carlo simulation, we consider a K-matrix model for a coupled-channel S-wave scattering system.

In the scaling regime, the phase shifts of the Ising model $\delta_{\phi,\sigma}$ in $1+1$ dimensions are shifted by a background phase $\delta_{\rm Ising} = \frac{\pi}{2}$ [28, 30, 31],

$$\delta_{\phi,\sigma} = \delta^{\rm Res}_{\phi,\sigma} - \delta_{\rm Ising}, \quad (38)$$

where $\delta^{\rm Res}$ represent the normal phase shift in which a resonance may appear at value of $\delta^{\rm Res} = \frac{\pi}{2}$. Thus, the unitarized t-matrix may be defined by

$$t_{\alpha\alpha} = -t^{\rm Res}_{\alpha\alpha} + i\theta(s-4m^2_\alpha)\frac{\sqrt{s}}{2k_\alpha},$$
$$t_{\alpha\beta} = -\theta(s-4m^2_\sigma)t^{\rm Res}_{\alpha\beta},$$

where $t-$ and $t^{\rm Res}$-matrix are parametrized by phase shifts $\delta_{\phi,\sigma}$, $\delta^{\rm Res}_{\phi,\sigma}$ and inelasticity η respectively. The t-matrix is related to the f-matrix defined in Eq.(25) by equation $t_{\alpha\beta} = \frac{\sqrt{s}}{2\sqrt{k_\alpha k_\beta}}f_{\alpha\beta}$. The unitarity relation of the

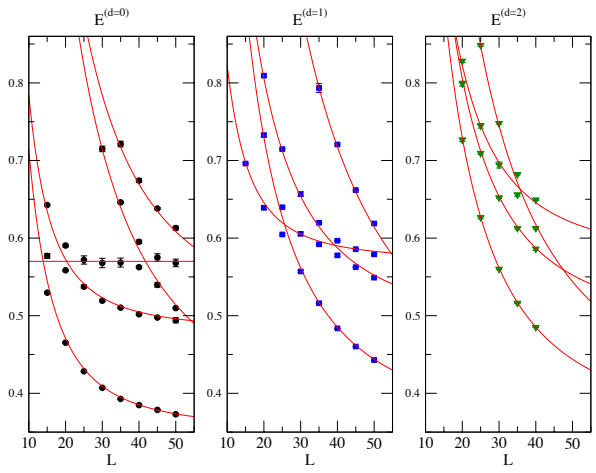

FIG. 3: The energy spectra of a coupled-channel Ising model as function of (L,d): (Left) $d=0$, (Middle) $d=1$ and (Right) $d=2$. The red curves represent (I) the energy spectra of a non-interacting pair of particles: $E^{(d)} = \sum_{i=\pm}\cosh^{-1}(\cosh m_{\phi,\sigma}+1-\cos p_i)$, where $p_\pm = \frac{2\pi}{L}n_\pm \pm \frac{\pi}{L}$, $n_+ + n_- = d$, and $(n_\pm, d)\in\mathbb{Z}$. The masses of ϕ,σ are given by $m_\phi \simeq 0.176, m_\sigma \simeq 0.240$; (II) the energy spectra of a stable resonance (no couplings between ρ and $2\phi, 2\sigma$ states: $g_{\rho\phi\phi} = g_{\rho\sigma\sigma} = 0$): $E^{(d)} = \cosh^{-1}(\cosh m_\rho + 1 - \cos P)$, where $m_\rho \simeq 0.57$.

t-matrix, $Im\left[t^{-1}(s)\right]_{\alpha\beta} = -\delta_{\alpha\beta}\theta(s-4m_\alpha^2)\frac{2k_\alpha}{\sqrt{s}}$, is guaranteed by the unitarity relation of the $t^{\rm Res}$-matrix. The Ising model suggestion is to parameterize a resonance coupling to both channels using a pole interfering with a polynomial in an S-wave K-matrix,

$$K_{\alpha\beta}(s) = \frac{g_\alpha g_\beta}{M^2-s} + \gamma^{(0)}_{\alpha\beta} + \gamma^{(1)}_{\alpha\beta}\, s + \ldots, \qquad (39)$$

where the inverse of the $t^{\rm Res}$-matrix is given by

$$\left[\left(t^{\rm Res}\right)^{-1}(s)\right]_{\alpha\beta} = \left[K^{-1}(s)\right]_{\alpha\beta} + \delta_{\alpha\beta}\, I_\alpha(s). \qquad (40)$$

Here $I_\alpha(s)$ is the Chew-Mandelstam form [32] whose imaginary part above threshold ($s > 4m_\alpha^2$) is the phase-space,

$$I_\alpha(s) = I_\alpha(0) - \frac{s}{\pi}\int_{4m_\alpha^2}^{\infty} ds' \sqrt{1-\frac{4m_\alpha^2}{s'}}\,\frac{1}{(s'-s)s'}. \qquad (41)$$

We have opted to subtract the integral once, and it is convenient to choose $I_\alpha(0)$ such that $\mathrm{Re}\, I_\alpha(M^2) = 0$ so that we have an amplitude which for real s near M^2 is close to the Breit-Wigner form with mass M.

Given an explicit model for the scattering amplitudes, we can solve Eq.(42) for the finite volume spectra in various volumes and total momenta $P = \frac{2\pi}{L}d, d\in\mathbb{Z}$.

$$\left(\frac{1}{f_{\mathcal{P}}^{\phi\phi}} + i + \cot\frac{p_\phi L+\pi d}{2}\right)\left(\frac{1}{f_{\mathcal{P}}^{\sigma\sigma}} + i + \cot\frac{p_\sigma L+\pi d}{2}\right) = \left(i+\cot\frac{p_\phi L+\pi d}{2}\right)\left(i+\cot\frac{p_\sigma L+\pi d}{2}\right)\frac{\left(f_{\mathcal{P}}^{\phi\sigma}\right)^2}{f_{\mathcal{P}}^{\phi\phi} f_{\mathcal{P}}^{\sigma\sigma}}. \qquad (42)$$

Eq.(42) is derived from Eq.(24) by replacing γk_α with p_α ($\alpha = \phi,\sigma$), where p_α is the relative momentum of two particles in a moving frame: $p_\alpha = \frac{p_{\alpha,1}-p_{\alpha,2}}{2}$ and $P = p_{\alpha,1} + p_{\alpha,2}$. To compensate for the ultraviolet cut-off effect from the finite lattice spacing, the dispersion relation $\cosh E = \cosh m + 1 - \cosh p$ [28] is used in this work, accordingly, in Eq.(42), the relative momenta of two particles in a moving frame p_α are solved by the equations

$$\begin{aligned} P &= p_{\alpha,1} + p_{\alpha,2}, \\ E^{(d)} &= \sum_{i=1,2}\cosh^{-1}\left(\cosh m_\alpha + 1 - \cos p_{\alpha,i}\right). \end{aligned}$$

The lattice dispersion relation and finite size effects are further discussed in Appendix B.

D. Data analysis

With the K-matrix model described in Section IV C, we can perform a global fitting method proposed in [13] to the spectra in Fig.3. For this purpose, we can minimize a function

$$\chi^2(\{a_i\}) = \sum_{E_n(L,d)} \frac{\left[E_n(L,d) - E_n^{\rm det}(L,d;\{a_i\})\right]^2}{\sigma(E_n(L,d))^2}, \qquad (43)$$

within the space of K-matrix parameters, $\{a_i\} = \{M, g_\phi, g_\sigma, \gamma^{(n)}\ldots\}$, where E_n denotes the energy levels from Monte Carlo simulation, and $E_n^{\rm det}$ are the solutions of Eq.(42).

Instead of establishing the resonance pole position in our toy model, the purpose of this work is to demonstrate (1) the methodology of extracting scattering amplitudes

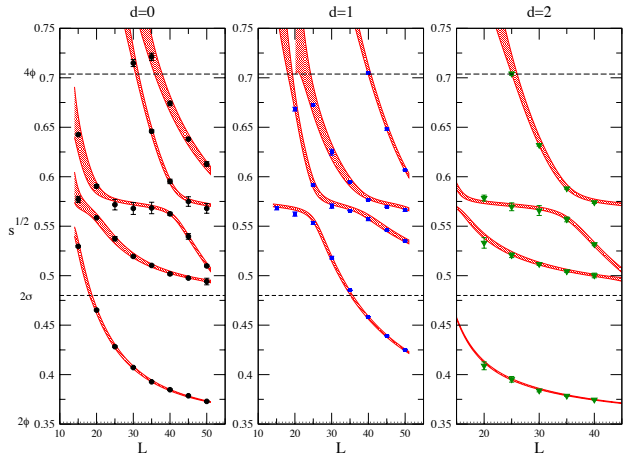

FIG. 4: The finite volume energy spectra from K-matrix model (red band) as function of (L, d), the spectra of K-matrix model are obtained by performing the fit on $d = 0$ lattice data below 4ϕ threshold only (black filled circles on the left). All the spectra in above three plots ($d = 0, 1, 2$) are presented in CM frame. The prediction of energy spectra from K-matrix model fit (red band) are also given for (Middle) $d = 1$ and (Right) $d = 2$ compared to the Monte Carlo simulation data for $d = 1$ (blue filled square) and $d = 2$ (green filled triangle) respectively. $\frac{\chi^2}{N_{dof}} = \frac{20.4}{31-9} = 0.93$.

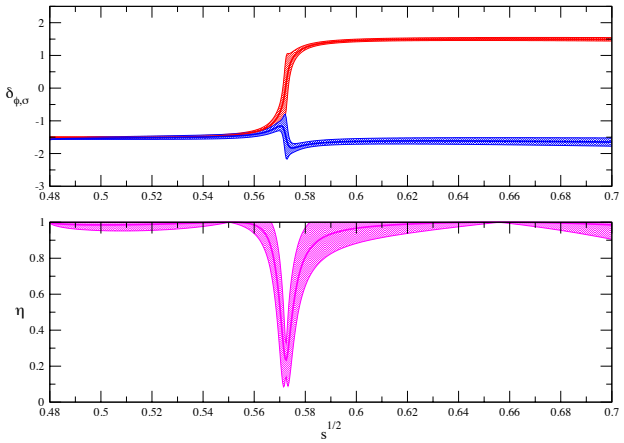

FIG. 5: The extracted phase shifts δ_ϕ(red), δ_σ(blue) and inelasticity η(purple).

from data of coupled-channel Monte Carlo simulations, (2) predictability of scattering amplitudes extracted from a set of lattice data, and (3) the validity of our formalism while taking into account of the finite size effect presented in Appendix B. Therefore, in this work, we choose to fit the spectra below 4ϕ threshold for $d = 0$ only, then for a consistency check, we compare our predicted spectra for $d = 1, 2$ to the spectra from the Monte Carlo simulation[2]. We show the spectra of K-matrix model (red bands) in Fig.4 with the comparison of spectra from the Monte Carlo simulation (filled black circles, filled blue squares and filled green triangles). The K-matrix we used in the fitting has nine free parameters, the polynomial of $\gamma^{(n)}$ is taken up to $\mathcal{O}(s^1)(n = 0, 1)$. The value of parameters we find from fitting read

$$M = 0.572(1), g_\phi = 0.064(4), g_\sigma = 0.060(4),$$
$$\gamma^{(0)}_{\phi\phi} = 0.3(1), \gamma^{(1)}_{\phi\phi} = -0.7(3), \gamma^{(0)}_{\phi\sigma} = 0.11(3),$$
$$\gamma^{(1)}_{\phi\sigma} = -0.3(1), \gamma^{(0)}_{\sigma\sigma} = -0.6(2), \gamma^{(1)}_{\sigma\sigma} = 1.5(5).$$

The extracted phase shifts δ_ϕ, δ_σ and inelasticity η are shown in Fig.5.

As demonstrated in the middle and the right plots in Fig.4, our predicted energy spectra from K-matrix model (red bands) for $d = 1, 2$ agree with the spectra from the Monte Carlo simulation (filled blue squares and filled green triangles) within a reasonable precision. Therefore, we accomplished our goals, (1) we proved that our formalism gives the consistent result in different moving frames while taking into account of finite size effect, and (2) we have shown that the global fitting method is a valid and fairly reliable means for extracting scattering amplitudes from Monte Carlo simulation data.

V. SUMMARY

Based on the Lippmann-Schwinger equation approach, in Section II and III, we first derived a generalized Lüscher's formula in 2D for two particles scattering in both the elastic and coupled-channel cases in moving frames. In Section IV, we presented a 2D coupled-channel scattering lattice model. The model simulates a two-coupled-channel resonant scattering system, in which a resonance couples to both channels. Next,

[2] A model-independent strategy of extracting phase shifts and inelasticity of a coupled-channel system has been discussed in [13], in which a set of simultaneous equations as the function of two phase shifts and one inelasticity can be solved by using three degenerate energy levels from different lattice volumes and momenta. However, finding three degenerate energy levels from limited number of lattice data points is still a difficult task in a realistic lattice simulation. Thus, as we stressed in Section IV D, the goal of this work is to demonstrate the validity and reliability of the global fitting method by parametrizing scattering amplitudes.

we performed Monte Carlo simulations on various finite lattice sizes and in different moving frames. The discrete finite-volume spectra were extracted by fitting two-particle correlation functions. Finally, we used the 2D generalized Lüscher's formula to extract the scattering amplitudes for the coupled-channel system from the discrete finite-volume spectra. We have shown that the global fitting method can be used to reliably extract scattering amplitudes from Monte Carlo simulation data. The finite size effects on the solution of the generalized Lüscher's formula were discussed in details in Section IV and Appendix B. We demonstrated that while taking into account of finite size effects, our formulae produce consistent results in different moving frames.

VI. ACKNOWLEDGMENTS

We thank Dru B. Renner, Robert G. Edwards and Han-Qing Zheng for useful discussions, and the special thanks go to Dru B. Renner for inspiration of this work and for his encouragement. We also thank David J. Wilson for carefully reading through this manuscript. PG acknowledges support from U.S. Department of Energy contract DE-AC05-06OR23177, under which Jefferson Science Associates, LLC, manages and operates Jefferson Laboratory.

Appendix A: One dimensional infinite sum

Let's consider the one dimensional infinite sum in Eq.(15),

$$\sum_{n\in\mathbb{Z}} e^{ik|x-x'-\gamma nL|}e^{i\frac{P}{2}nL}, \tag{A1}$$

where $P=\frac{2\pi}{L}d, d\in\mathbb{Z}$.

In the region which we are interested in: $|x|>|x'|$ and $|x-x'|<\gamma L$, Eq.(A1) can be rewritten to

$$e^{ik|x|}\sum_{\mathcal{P}=\pm} Y_{\mathcal{P}}(x)Y_{\mathcal{P}}(x')J^*_{\mathcal{P}}(kx') + \sum_{n\in\mathbb{Z}}^{n\neq 0} e^{ik|\gamma nL|}e^{i\frac{P}{2}nL}\sum_{\mathcal{P}=\pm} Y_{\mathcal{P}}(n)Y_{\mathcal{P}}(x)J_{\mathcal{P}}(kx)\sum_{\mathcal{P}'=\pm} Y_{\mathcal{P}'}(n)Y_{\mathcal{P}'}(x')J^*_{\mathcal{P}'}(kx'). \tag{A2}$$

With the help of equations

$$\sum_{n\in\mathbb{Z}}^{n\neq 0} e^{ik|\gamma nL|}e^{i\frac{P}{2}nL}Y_+(n) = \frac{\cos\frac{PL}{2}-e^{i\gamma kL}}{\cos\gamma kL-\cos\frac{PL}{2}}, \qquad \sum_{n\in\mathbb{Z}}^{n\neq 0} e^{ik|\gamma nL|}e^{i\frac{P}{2}nL}Y_-(n) = i\frac{\sin\frac{PL}{2}}{\cos\gamma kL-\cos\frac{PL}{2}},$$

where the infinite sums are performed by using the property of polylogarithmic function $Li_0(x)=\sum_{n=1}^{\infty}x^n=\frac{x}{1-x}$, thus, we find

$$\sum_{n\in\mathbb{Z}} e^{ik|x-x'-\gamma nL|}e^{i\pi nd} = \sum_{\mathcal{P}=\pm} Y_{\mathcal{P}}(x)Y_{\mathcal{P}}(x')J^*_{\mathcal{P}}(kx')\left[e^{ik|x|}-\left(1-i\cot\frac{\gamma kL+\pi d}{2}\right)J_{\mathcal{P}}(kx)\right], \tag{A3}$$

for $|x|>|x'|$ and $|x-x'|<\gamma L$.

Appendix B: Lattice dispersion relation

For the determination of the lattice spectrum at a precise level, the finite size effect has to be taken into consideration by using the lattice dispersion relation [28]

$$\cosh\sqrt{s} = \cosh E^{(d)} - (1-\cos P), \tag{B1}$$

where $E^{(d)}$ and $\sqrt{s}$ are the total energy of system in moving frames and the CM frame respectively, and the total momentum of system is given by $P=\frac{2\pi}{L}d, d\in\mathbb{Z}$. In the limit of vanishing lattice spacing, Eq.(B1) reduces to the relativistic dispersion relation: $E^{(d)}=\sqrt{s+P^2}$.

The relative momentum of two particles $p=\frac{p_1-p_2}{2}$ in a moving frame ($p_1+p_2=P$) is related to the relative momentum of two particles $k=\frac{k_1-k_2}{2}$ in the CM frame ($k_1+k_2=0$) by Lorentz transformation relation $p=\gamma k$. In the limit of vanishing lattice spacing, the Lorentz contraction factor γ is given by $\gamma=\frac{E^{(d)}}{\sqrt{s}}$. However, due to the ultraviolet cut-off effect from finite lattice spacing, the definition of the Lorentz contraction factor $\gamma=\frac{E^{(d)}}{\sqrt{s}}$ is inconsistent with lattice dispersion relation Eq.(B1). This inconsistency leads to the large discrepancies of phase shifts and inelasiticy computed in different frames. To resolve this problem, we may use the relation $p=\gamma k$ to rewrite Eq.(19), Eq.(24) and Eq.(26) to

$$\cot\delta_{\mathcal{P}} + \cot\frac{pL+\pi d}{2} = 0, \tag{B2}$$

for single channel scattering, and

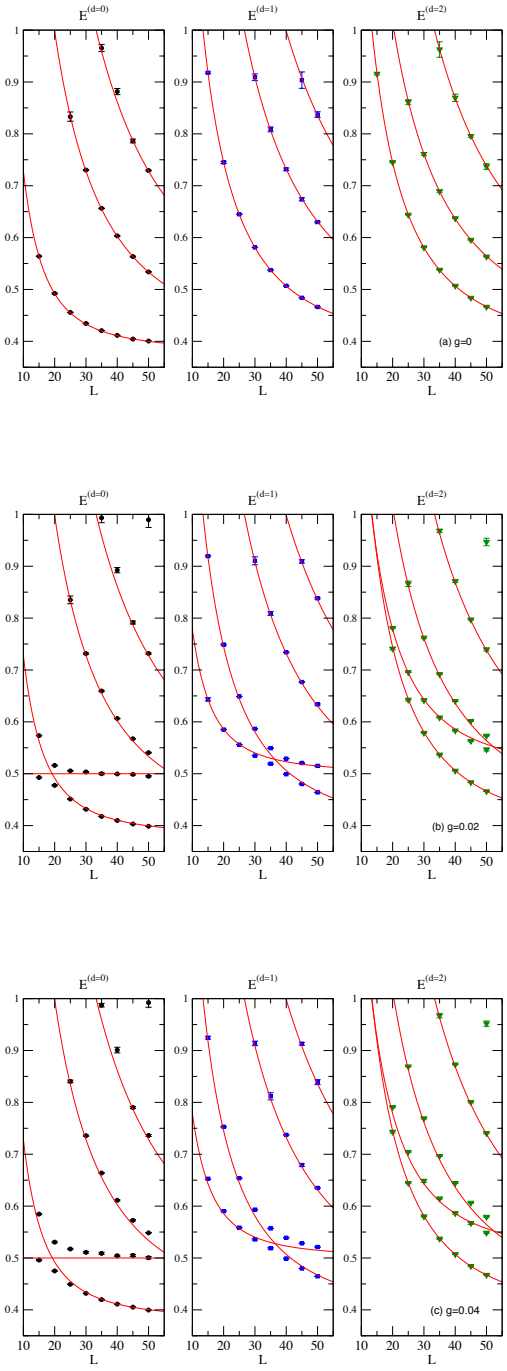

FIG. 6: The energy spectra of single channel Ising model [28] as function of (L, d) for (a) $g = 0$ (Upper panel), (b) $g = 0.02$ (Middle panel) and (c) $g = 0.04$ (Lower panel) respectively. In each panel, from left to right, each individual plot is related to $d = 0$ (black filled circles), 1 (red filled squares) and 2 (green filled triangles) respectively. The red curves represent (I) the energy spectra of a non-interacting pair of particles: $E^{(d)} = \sum_{i=\pm} \cosh^{-1}(\cosh m + 1 - \cos p_i)$, where $p_\pm = \frac{2\pi}{L} n_\pm \pm \frac{\pi}{L}$, $n_+ + n_- = d$ and $(n_\pm, d) \in \mathbb{Z}$; (II) the energy spectra of a stable resonance: $E^{(d)} = \cosh^{-1}(\cosh m_\rho + 1 - \cos P)$, where $m_\rho \simeq 0.5$.

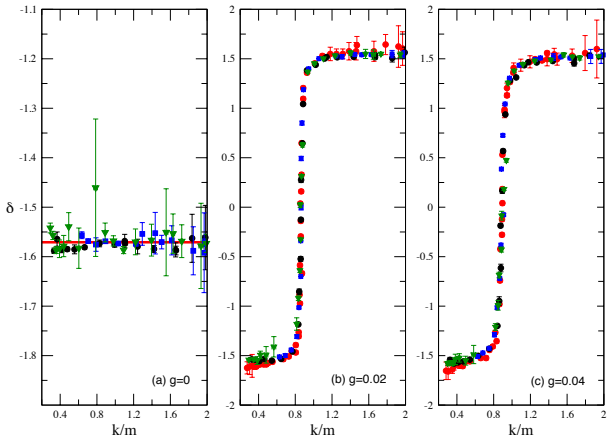

FIG. 7: The phase shifts of single channel Ising model [28] for (a) $g = 0$ (Left), (b) $g = 0.02$ (Middle) and (c) $g = 0.04$ (Right) respectively. The red line in left plot labels the theoretical expectation $\delta_{\rm Ising} = -\frac{\pi}{2}$ for non-interacting case (a) $g = 0$. The red filled circles, black filled circles, blue filled squares and green filled triangles represent the result in Fig.6 of [28], and our results for $d = 0, 1, 2$ respectively.

.

$$\left(\frac{1}{f_{\mathcal{P}}^{\phi\phi}} + i + \cot\frac{p_\phi L + \pi d}{2}\right)\left(\frac{1}{f_{\mathcal{P}}^{\sigma\sigma}} + i + \cot\frac{p_\sigma L + \pi d}{2}\right) = \left(i + \cot\frac{p_\phi L + \pi d}{2}\right)\left(i + \cot\frac{p_\sigma L + \pi d}{2}\right)\frac{\left(f_{\mathcal{P}}^{\phi\sigma}\right)^2}{f_{\mathcal{P}}^{\phi\phi} f_{\mathcal{P}}^{\sigma\sigma}}.$$

or

$$\eta_{\mathcal{P}}\,(-1)^d = \frac{\cos\left(\frac{p_\phi+p_\sigma}{2}L + \delta_{\mathcal{P}}^{\phi} + \delta_{\mathcal{P}}^{\sigma}\right)}{\cos\left(\frac{p_\phi-p_\sigma}{2}L + \delta_{\mathcal{P}}^{\phi} - \delta_{\mathcal{P}}^{\sigma}\right)}, \qquad \text{(B3)}$$

for coupled channel scattering, respectively. In Eq.(B2), Eq.(42) and Eq.(B3), the relative momentum of two particles $p = \frac{p_1-p_2}{2}$ is solved by equations

$$\begin{aligned} P &= p_1 + p_2, \\ E^{(d)} &= \sum_{i=1,2} \cosh^{-1}\left(\cosh m + 1 - \cos p_i\right). \end{aligned} \qquad \text{(B4)}$$

So that, rather than solving Eq.(19), Eq.(24) and Eq.(26) with the Lorentz contraction factor given by $\gamma = \frac{E^{(d)}}{\sqrt{s}}$, we use Eq.(B2) and Eq.(42) with the solution of relative momentum of two particles given by Eq.(B4) for single and coupled-channel scattering respectively in this work.

As a simple demonstration how the above proposal works, let's consider a non-interacting two-particle system in $1+1$ dimensions. Two particles in an arbitrary moving frame, $P = \frac{2\pi}{L}d$, have individual momenta $p_\pm = \frac{2\pi}{L}n_\pm \pm \frac{\pi}{L}$ respectively, where $n_+ + n_- = d$ and $(n_\pm, d) \in \mathbb{Z}$. So that we get a relation: $\frac{pL+\pi d}{2} = n_+\pi + \frac{\pi}{2}$, where $p = \frac{p_+-p_-}{2}$ is the relative momentum of two-particle system. Using Eq.(B2), we conclude that the phase shift of two non-interacting particles is given by $\delta = \delta_{\rm Ising} = -\frac{\pi}{2}$. This conclusion derived from Eq.(B2) holds in all the moving frames.

As an more quantitative example, we generalize the single channel Ising model computed in CM frame in [28] to the moving frames, we compute the three sets of models [28] (see Table 1 in [28]) for three different moving frames: $d = 0, 1, 2$. Three models are labeled by coupling constants: (a) $g = 0$, (b) $g = 0.02$ and (c) $g = 0.04$, all the parameters are given by Table 1 in [28]. The measured energy levels for three models ($g = 0, 0.02, 0.04$) and three moving frames ($d = 0, 1, 2$) are shown in Fig.6, the extracted phase shifts by using Eq.(B2) along with the solution of relative momentum of two particles from

Eq.(B4) are shown in Fig.7. Fig.7 demonstrates the consistent calculation of phase shift from different moving frames by using Eq.(B2) along with Eq.(B4).

[1] M. Lüscher, Nucl. Phys. B **354**, 531 (1991).
[2] K. Rummukainen, S. Gottlieb, Nucl. Phys. B **450**, 397 (1995).
[3] C.-J.D. Lin, G. Martinelli, C. T. Sachrajda and M. Testa, Nucl. Phys. B **619**, 467 (2001).
[4] N. H. Christ, C. Kim and T.Yamazaki, Phys. Rev. D **72**, 114506 (2005).
[5] V. Bernard, Ulf-G. Meißner and A. Rusetsky, Nucl. Phys. B **788**, 1 (2008).
[6] V. Bernard, M. Lage, Ulf-G. Meißner and A.Rusetsky, JHEP **0808**, 024 (2008).
[7] S. He, X. Feng, C. Liu, JHEP **0507**, 011 (2005).
[8] M. Lage, Ulf-G. Meißner and A. Rusetsky, Phys. Lett. B **681**, 439 (2009)
[9] M. Döring, Ulf-G. Meißner,E. Oset and A. Rusetsky, Eur. Phys. J. A **47**, 139 (2011)
[10] S. Aoki *et al.* [HAL QCD Collaboration], Proc. Japan Acad. B **87**, 509 (2011)
[11] R. A. Briceno and Z. Davoudi, arXiv:1204.1110 [hep-lat].
[12] M. T. Hansen and S. R. Sharpe, Phys. Rev. D **86**, 016007 (2012)
[13] P. Guo, J. Dudek, R. Edwards, A. P. Szczepaniak, [arXiv:1211.0929 [hep-lat]].
[14] C. Michael, Nucl. Phys. B **259**, 58 (1985).
[15] M. Luscher and U. Wolff, Nucl. Phys. B **339**, 222 (1990).
[16] B. Blossier, M. Della Morte, G. von Hippel, T. Mendes and R. Sommer, JHEP **0904**, 094 (2009)
[17] J. J. Dudek *et al.* (Hadron Spectrum Collaboration), Phys. Rev. D **82**, 034508 (2010).
[18] R. G. Edwards, J. J. Dudek, D. G. Richards, and S. J. Wallace, Phys. Rev. D **84**, 074508 (2011).
[19] S. Aoki *et al.* [CP-PACS Collaboration], Phys. Rev. D **76**, 094506 (2007)
[20] K. Sasaki, and N. Ishizuka, Phys. Rev. D **78**, 014511 (2008).
[21] X. Feng, K. Jansen, and D. B. Renner, Phys. Rev. D **83**, 094505 (2011).
[22] J. J. Dudek *et al.* (Hadron Spectrum Collaboration), Phys. Rev. D **83**, 071504 (2011).
[23] S. R. Beane *et al.* (NPLQCD Collaboration), Phys. Rev. D **85**, 034505 (2012).
[24] C. B. Lang, D. Mohler, S. Prelovsek and M. Vidmar, Phys. Rev. D **84**, 054503 (2011).
[25] S. Aoki *et al.* [CS Collaboration], Phys. Rev. D **84**, 094505 (2011)
[26] J. J. Dudek *et al.* (Hadron Spectrum Collaboration), Phys. Rev. D **86**, 034031 (2012).
[27] J. J. Dudek, R. G. Edwards and C. E. Thomas, Phys. Rev. D **87**, 034505 (2013).
[28] C. R. Gattringer and C. B. Lang, Nucl. Phys. B **391**, 463 (1993).
[29] N. Ishii *et al.* HAL QCD Collaboration, Phys. Lett. B **712**, 437 (2012).
[30] M. Sato, T. Miwa and M. Jimbo, Proc. Japan Acad **53**, Ser. A, 6 (1977).
[31] B. Berg, M. Karowski and P. Weisz, Phys. Rev. D **19**, 2477 (1979).
[32] J. L. Basdevant and E. L. Berger, Phys. Rev. D **16**, 657 (1977).